J Bone Miner Metab (2012) 30:31–39
DOI 10.1007/s00774-011-0292-6

ORIGINAL ARTICLE

Elbow loading promotes longitudinal bone growth of the ulna and the humerus

Ping Zhang · Hiroki Yokota

Received: 9 March 2011 / Accepted: 5 June 2011 / Published online: 6 July 2011

Abstract Mechanical stimulation plays a critical role in bone development and growth. In view of recently recognized anabolic responses promoted by a joint-loading modality, we examined the effects of elbow loading on longitudinal growth of the ulna and the humerus. Using a custom-made piezoelectric loader, the left elbow of growing C57/BL/6 female mice was given daily 5-min bouts of dynamic loading for 10 days. The right forelimbs of those mice served as contralateral controls, and the limbs of non-treated mice were used as age-matched controls. The effects of elbow loading were evaluated through measurement of bone length, weight, bone mineral density (BMD), and bone mineral content (BMC), as well as mRNA expression levels of load-sensitive transcription factors such as c-fos, egr1, and atf3. The results revealed that the humerus was elongated by 1.2% compared to the contralateral and age-matched controls (both $p < 0.001$), while the ulna had become longer than the contralateral control (1.7%; $p < 0.05$) and the age-match control (3.4%; $p < 0.001$). Bone lengthening was associated with increases in bone weight, BMD and BMC. Furthermore, the mRNA levels of the selected transcription factors were elevated in the loaded ulna and humerus. Interestingly, the increase was observed not only at the elbow but also at the wrist and shoulder in the loaded limb. The present study demonstrates that joint loading is potentially useful for stimulating bone lengthening and treating limb length discrepancy.

Keywords Elbow loading · Bone length · Ulna · Humerus

Introduction

Mild differences between the two sides of the body may simply represent variations with no apparent clinical problems. However, differences in leg length above a normal variation of 5–15 mm are called limb length discrepancies and potentially induce various medical symptoms including hip and low back pain, arthritis, and overuse injuries such as tendonitis [1–3]. In order to reduce lateral ground reaction forces that predominantly act on the short limb, a common non-surgical practice is the use of shoe lifts. When used inappropriately, however, shoe lifts can create additional pain [4]. In severe discrepancy cases, surgical treatments such as shortening the long leg and lengthening the short leg are performed [5–7]. It is controversial as to how and when either of these invasive procedures should be performed especially for growing children [8–11]. To evaluate the possibility of employing mechanical loading for bone lengthening, we focused here on examining a recently developed loading modality—pulsating joint loading. Development of non-invasive mechanical loading that is free of pharmacological side-effects may also contribute to treating short stature in children caused by birth defect

P. Zhang
Department of Pediatrics,
Indiana University School of Medicine,
Indianapolis, IN 46202, USA

H. Yokota (✉)
Department of Biomedical Engineering,
Indiana University-Purdue University Indianapolis,
SL220C, 723 West Michigan Street,
Indianapolis, IN 46202, USA
e-mail: hyokota@iupui.edu

syndromes, hormonal deficiency or many other reasons [12–14].

Mechanical stimulation is essential for maintenance of load-bearing tissues including trabecular and cortical bone as well as articular cartilage [15, 16]. It is important to note that load-driven effects on bone and cartilage differ significantly depending on loading procedures and mechanical conditions. For instance, sustained (static) distraction is shown to accelerate the rate of longitudinal growth but sustained compression slows its growth [17–19]. Furthermore, compressive axial loading to the ulna has been reported to suppress longitudinal growth, although it increases anabolic responses on the cortical surfaces [20, 21]. To our knowledge, the effects of tensile dynamic loading on longitudinal bone growth have not been fully evaluated.

We recently developed a series of joint-loading modalities such as elbow loading [22], knee loading [23–25], and ankle loading [26], in which dynamic mechanical loads are laterally applied to the elbow, knee, and ankle, respectively. Such joint loading has been shown to increase the thickness and the cortical area of the cross-section of long bones [27, 28]. Using knee loading, it was reported that the lengths of the femur and the tibia were increased [29]. In the hypertrophic zone of the growth plate in the proximal tibia, the number of chondrocytes and their cellular height were elevated. Thus, joint loading is potentially useful to lengthen long bones in the hindlimb and the growth plate at the loading site exhibits morphological alterations; however, no studies have been conducted for the forelimb. Furthermore, little is known about potential alterations in gene expression not only in the loaded joint but also at the other end of long bones (e.g., the wrist and shoulder for elbow loading), which are not directly under mechanical loading.

In the current study the specific questions addressed are: does elbow loading increase the longitudinal length of the humerus and the ulna in the forelimb? Are stress-sensitive transcription factors activated in the directly loaded elbow (i.e., proximal ulna and distal humerus) and the non-directly loaded wrist and shoulder (i.e., distal ulna and proximal humerus)? We hypothesized that lateral loads applied with elbow loading would increase longitudinal bone growth in the forelimb with load-driven gene activation not only at the elbow but also at the wrist and shoulder. Elbow loading was chosen to identify a potentially differential effect of tensile loads compared to compressive loads in previously reported ulna-loading studies, where the longitudinal growth of the ulna was suppressed [20, 21]. Loading experiments were conducted using female mice. We determined bone length, weight, total bone mineral density (BMD), and total bone mineral content (BMC) of the humerus and the ulna. We examined the mRNA expression levels of three transcription factors as representative, stress-sensitive genes.

Materials and methods

Animals

Experimental procedures were approved by the Indiana University Animal Care and Use Committee and were in compliance with the Guiding Principles in the Care and Use of Animals endorsed by the American Physiological Society. Thirty C57/BL/6 female mice, ~8 weeks of age (Harlan Sprague-Dawley, Inc., Indianapolis, IN, USA), were used. Four to five mice were housed per cage and were fed with mouse chow and water ad libitum. The animals were allowed to acclimate for 2 weeks before the experiment. The mice were randomly divided into two groups: the loading group ($n = 24$) and the age-matched control group ($n = 6$). Twenty-one mice were used for histology and nine mice for molecular analysis.

Experimental design

In the loading group, mice were mask-anesthetized using 1.5% isoflurane and received loads to the left elbow in the lateral-medial direction with the custom-made piezoelectric mechanical loader. Loads were 0.5 N at 5 Hz and given for 5 min per day for 10 days (Fig. 1a, b). The lateral and the medial sides of the ulna and humerus were in contact with the loading rod and the stator, respectively. We chose a forelimb configuration that made the right angle (90°) between the ulna and the humerus, since in this position the forelimb was relaxed and stably immobilized (Fig. 1c). To position the elbow properly for loading, the lower end of the loading rod and the upper end of the supporter (nylon screw) were designed to form a pair of semi-spherical cups. The olecranon process and coronoid process of the ulna together with the ulnar tuberosity, and medial and lateral epicondyles of the humerus were confined in the cups. The tip of the loader had a contact surface of 3 mm in diameter. To avoid a local stress concentration between the elbow and the loader, both the loading surface and supporter were covered with silicon rubber. The right elbow was used as a sham loading control (contralateral control), which was placed under the loader with no dynamic loading. In the age-matched control group, the same procedure was applied without application of lateral loads.

For measurements of bone length, weight, BMD, and BMC, mice were sacrificed 2 weeks after the last loading, and all ulnae and humeri were harvested. The samples were

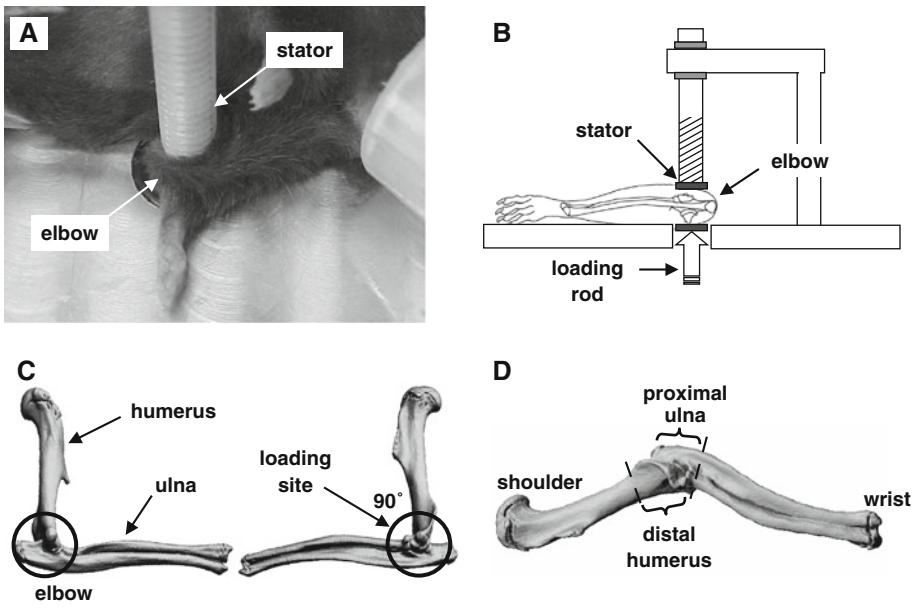

Fig. 1 Elbow loading. **a** Left elbow on the loading table. **b** Schematic diagram of the loading mechanism. **c** Micro-CT images showing the forelimb position for loading and the loading site. **d** Four regions employed for mRNA expression analysis, including the proximal ulna, distal ulna (wrist), distal humerus, and proximal humerus (shoulder)

cleaned of soft tissue and fixed in 10% neutral-buffered formalin. For determination of the mRNA levels of the selected genes, the bone samples were harvested 1 h after the third loading bout.

Measurements of bone length and weight

In order to achieve a reproducible procedure for measurements of bone length and weight, the samples stored in 10% neutral-buffered formalin were gently wrapped with soft, clean wipers and the solution around the sample was wiped out. Bone length was measured using a digital caliper with a resolution of 1/100 mm (Mitutoyo Corporation). The humerus length was defined from the proximal end of the humoral head to the distal humoral epicondyle, while the ulna length was defined from the proximal end of the olecranon process to the distal ulna junction with the wrist [21, 30]. Bone wet weight was determined immediately after length measurements with an electronic balance (Mettler Toledo Scaler, Switzerland) [31].

Microcomputed tomography (Micro-CT) imaging and determination of BMD and BMC

Micro-CT imaging was performed using a desktop μCT-20 (Scanco Medical AG, Auenring, Switzerland). The harvested forelimb was placed in a plastic tube filled with 70% ethanol and centered in the gantry of the imaging device. A series of cross-sectional images were captured at 30-μm resolution [25]. Using the procedure described previously, the BMD and BMC of an entire ulna and humerus were determined with a PIXImus densitometer (version 1.4, GE Medical System Lunar) [32, 33]. Using pQCT (XCT Research SA Plus), the BMD and BMC of the proximal ulna (15% from the proximal end of the ulna) and its midshaft (50% from the proximal end of the ulna) were also determined focusing on the section with 2 mm in length.

RNA isolation and real-time polymerase chain reaction (PCR)

For determination of the selected mRNA levels, 4 segments of bone samples including the region of articular cartilage were harvested at 1 h after the third loading bout: the proximal ulna, distal ulna, proximal humerus, and the distal humerus. Each of the samples was approximately one-fifth of a whole ulna or humerus (Fig. 1d). Soft surrounding tissues were dissected out from the samples and were ground with a mortar and pestle in an RNeasy plus lysis buffer. Tissue debris was removed using a QIA shredder spin column (Qiagen), and total RNA was isolated using a standard procedure with an RNeasy Plus Mini Kit (QIAGEN). Using ~50 ng of total RNA, reverse transcription was conducted with high capacity cDNA reverse transcription kits (Applied Biosystems).

Quantitative real-time PCR was performed using ABI 7500 with a Power SYBR Green PCR Master Mix Kit (Applied Biosystems). The mRNA levels of three transcription factors (c-fos: fbj osteosarcoma oncogene; egr1: early growth response 1; and atf3: activating transcription factor 3) were determined using the PCR primers listed in Table 1 with gapdh as an internal control. The mRNA levels were first calibrated using the gapdh mRNA levels. Then, the mRNA levels of the loaded samples were normalized by the mRNA levels of the contralateral samples to

Table 1 Real-time PCR primers used in the study

Gene	Forward primer	Backward primer
c-fos	5′-AGGCCCAGTGGCTCAGAGA-3′	5′-CCAGTCTGCTGCATAGAAGGAA-3′
egr1	5′-TCCGTTCCACCTGCTTTCC-3′	5′-GGAGAAAAGGTCGCTGTC-3′
atf3	5′-CGAAGACTGGAGCAAAATGATG-3′	5′-CAGGTTAGCAAAATCCTCAAATAC-3′
gapdh	5′-TGCACCACCAACTGCTTAG-3′	5′-GGATGCAGGGATGATGTTC-3′

derive relative mRNA changes. If the relative mRNA change is one, elbow loading does not have an effect on mRNA abundance.

Statistical analysis

The data were expressed as mean ± SD. Statistical significance among the loading and the age-matched groups was examined using one-way ANOVA. For pair-wise comparisons, a post hoc test was conducted using Fisher's 'protected least significant difference'. A paired *t* test was employed to evaluate statistical significance between the loaded and control samples. The relative parameters for length and weight were calculated as $([L - C]/C \times 100$ in %), where $L =$ 'loaded' and $C =$ 'control'. All comparisons were two-tailed and statistical significance was assumed for $p < 0.05$.

Results

During the loading experiment no bruising or other damage was detected at the loading site, and mice did not show weight loss or diminished food intake after loading.

Load-driven bone lengthening and weight increase

Elbow loading lengthened the humerus and the ulna (Fig. 2). In the humerus, the longitudinal length was increased by 1.3% from 11.19 ± 0.08 mm (contralateral control) to 11.32 ± 0.10 mm (loading) ($p < 0.001$). In the ulna, it was elevated by 1.7% from 13.03 ± 0.24 mm (contralateral control) to 13.25 ± 0.23 mm (loading) ($p < 0.05$). Compared to age-matched controls, elbow loading increased the longitudinal length by 1.2% (humerus, $p < 0.001$) and by 3.4% (ulna, $p < 0.001$).

Elbow loading also increased bone weight (Fig. 3). The humerus weight was increased by 6.8% from 24.12 ± 1.18 mg (contralateral control) to 25.76 ± 1.28 mg (loading) ($p < 0.001$). The ulna weight was changed by 10.3% from 15.17 ± 0.91 mg (contralateral control) to 16.74 ± 0.81 mg (loading) ($p < 0.001$). Furthermore, compared to age-matched controls, the humerus weight was increased by 8.7% ($p < 0.001$) and the ulna weight by 13.2% ($p < 0.001$).

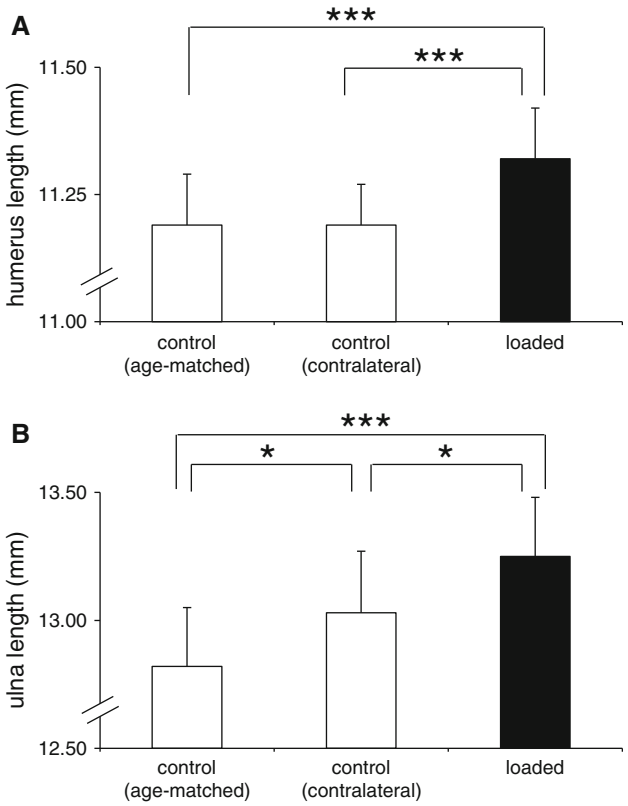

Fig. 2 Effects of elbow loading on bone length. The results are expressed as mean ± SD. The *single* and *triple asterisks* indicate $p < 0.05$ and $p < 0.001$, respectively. **a** Humerus length. **b** Ulna length

Load-driven increase in BMD and BMC

In response to elbow loading, we observed an increase in BMD and BMC in the humerus and ulna (Figs. 4, 5). The BMD increased from 0.0358 ± 0.001 g/cm^2 (contralateral control) to 0.0374 ± 0.0013 g/cm^2 (loading) in the humerus ($p < 0.001$) and from 0.0247 ± 0.0013 g/cm^2 (contralateral control) to 0.0265 ± 0.0008 g/cm^2 (loading) in the ulna ($p < 0.001$). In addition, the BMC of the humerus increased from 0.0079 ± 0.0004 g (contralateral control) to 0.0087 ± 0.0007 g (loading, $p < 0.001$), and the BMC of the ulna increased from 0.0051 ± 0.0006 g (contralateral control) to 0.0059 ± 0.0006 g (loading, $p < 0.01$). The load-driven increases in BMD and BMC were also statistically significant in the humerus and ulna to the age-matched control group.

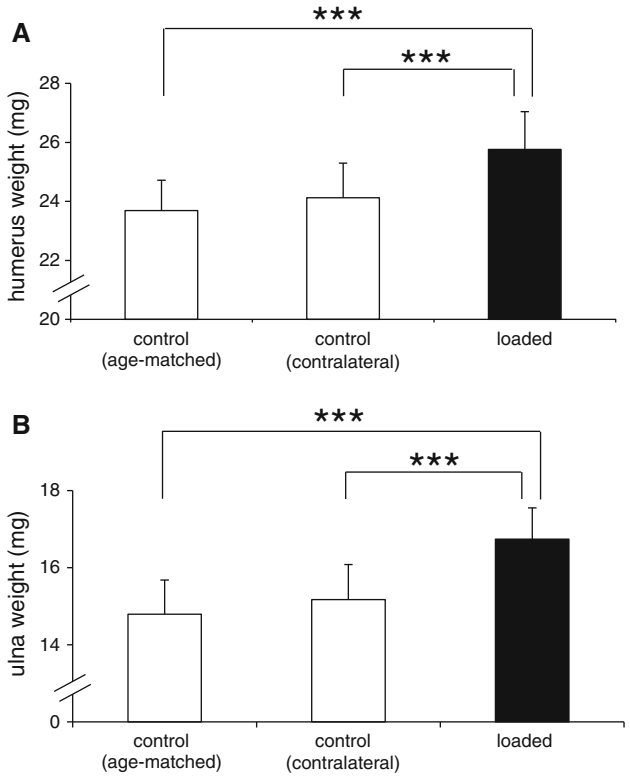

Fig. 3 Effects of elbow loading on bone weight. The results are expressed as mean ± SD. The *triple asterisk* indicates $p < 0.001$. **a** Humerus weight. **b** Ulna weight

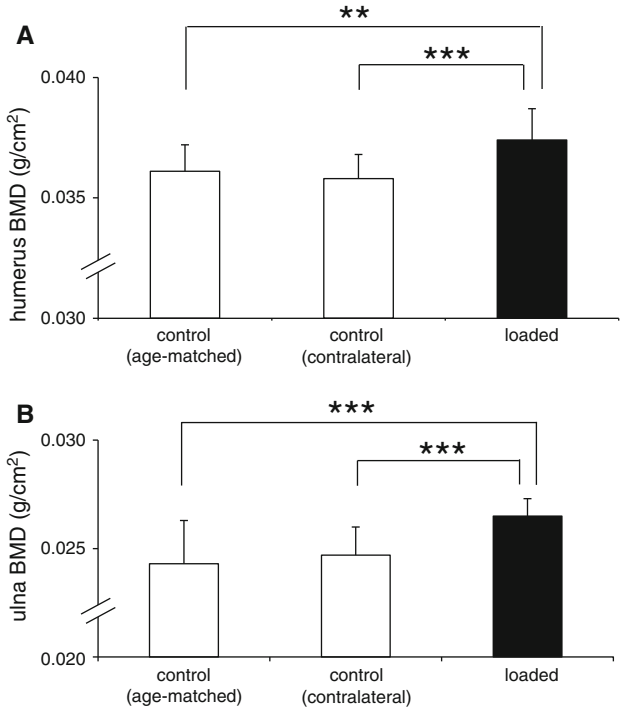

Fig. 4 Effects of elbow loading on BMD of the humerus and ulna. The results are expressed as mean ± SD. The *double* and *triple asterisks* indicate $p < 0.01$ and $p < 0.001$, respectively. **a** Effects on humerus BMD. **b** Effects on ulna BMD

Comparison of loading effects on the humerus and ulna

The amount of changes in response to elbow loading was not identical in the humerus and ulna. To further quantify responsiveness to elbow loading in these two bones, the load-driven change in bone length and weight was evaluated by calculating percentage increase to the value of the contralateral control. The result revealed that the ulna was more responsive to elbow loading than the humerus both for bone lengthening ($p < 0.01$), and weight increase ($p < 0.05$) (Fig. 6).

Alterations of cortical and trabecular bone in the proximal and midshaft ulna

Focusing on the ulna, which was more responsive than the humerus to load-driven bone lengthening and weight increase, we determined changes in geometry and BMC of cortical and trabecular bone (Fig. 7). In the middle position (50% of the length of the ulna from its proximal end), the cross-sectional areas of cortical bone and trabecular bone in the loaded samples were larger than those in the contralateral controls ($p < 0.05$). The BMC was also increased in the middle position ($p < 0.05$). In the proximal position (i.e., loading site), the cross-sectional areas and BMC were

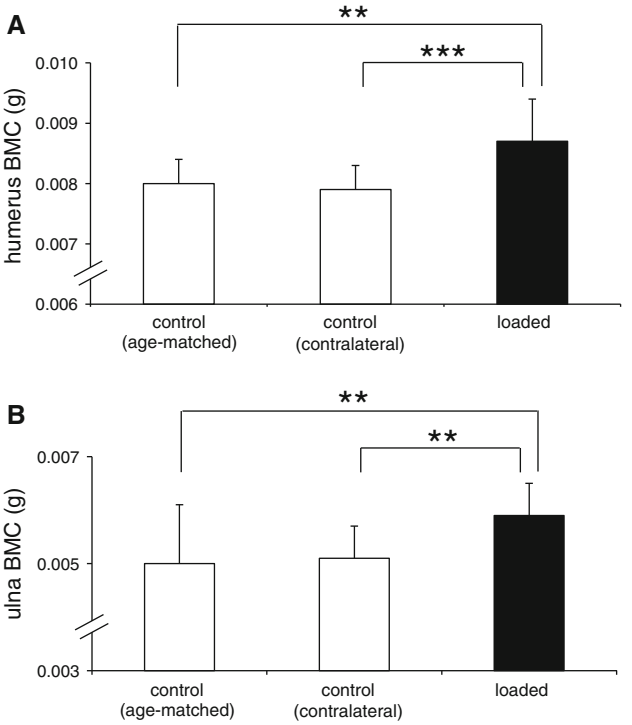

Fig. 5 Effects of elbow loading on BMC of the humerus and ulna. The results are expressed as mean ± SD. The *double* and *triple asterisks* indicate $p < 0.01$ and $p < 0.001$, respectively. **a** Effects on humerus BMC. **b** Effects on ulna BMC

elevated both in cortical bone and trabecular bone; however, the increases were not statistically significant.

Elevated mRNA levels of c-fos, egr-1, and atf3 in the elbow, wrist, and shoulder

Compared to the contralateral controls, elbow loading elevated the mRNA levels of the selected stress-responsive transcription factors (Fig. 8). At the loading site (distal humerus and proximal ulna), three early response genes (c-fos, egr-1, and atf3) were significantly upregulated. For instance, the load-drive fold change was 4.5 (c-fos), 4.0 (egr-1), and 6.0 (atf3) in the proximal ulna, and 2.9 (c-fos), 3.1 (egr-1), and 3.8 (atf3) in the distal humerus. Interestingly, upregulation of these mRNA levels was also observed in the distal ulna (wrist) and the proximal humerus (shoulder), which did not receive direct loading. The increases in the non-directly loaded samples were significantly smaller than in the directly loaded samples. Furthermore, the increases in the mRNA levels were higher in the ulna than the humerus.

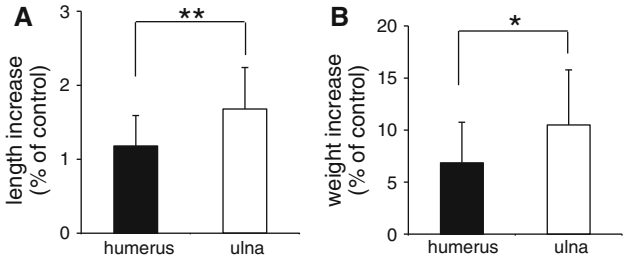

Fig. 6 Comparison of the increases in bone length and weight in the humerus and the ulna. **a** Increases in bone length normalized by the control value (percentage of contralateral control). **b** Increases in bone weight normalized by the control value (percentage of contralateral control)

Discussion

The present study demonstrates that elbow loading (1,500 daily cycles for 10 days) stimulates longitudinal bone growth in the humerus and the ulna. Compared to the contralateral controls, longitudinal length was increased on average by 1.2% (humerus) and 1.7% (ulna). Compared to the age-matched controls, these increases were 1.2% (humerus) and 3.4% (ulna). Bone weight, BMD and BMC were also elevated both in the humerus and the ulna. Unlike ulna bending that induces anabolic responses but shortens the ulna, the results here support the notion that elbow loading not only activates anabolic responses throughout the forelimb but also lengthens the ulna and the humerus. The ulna exhibited greater increases in all measurements than the humerus, including bone length and weight. We did not observe any load-driven damage in the subchondral bone and the articular cartilage in the humerus and ulna.

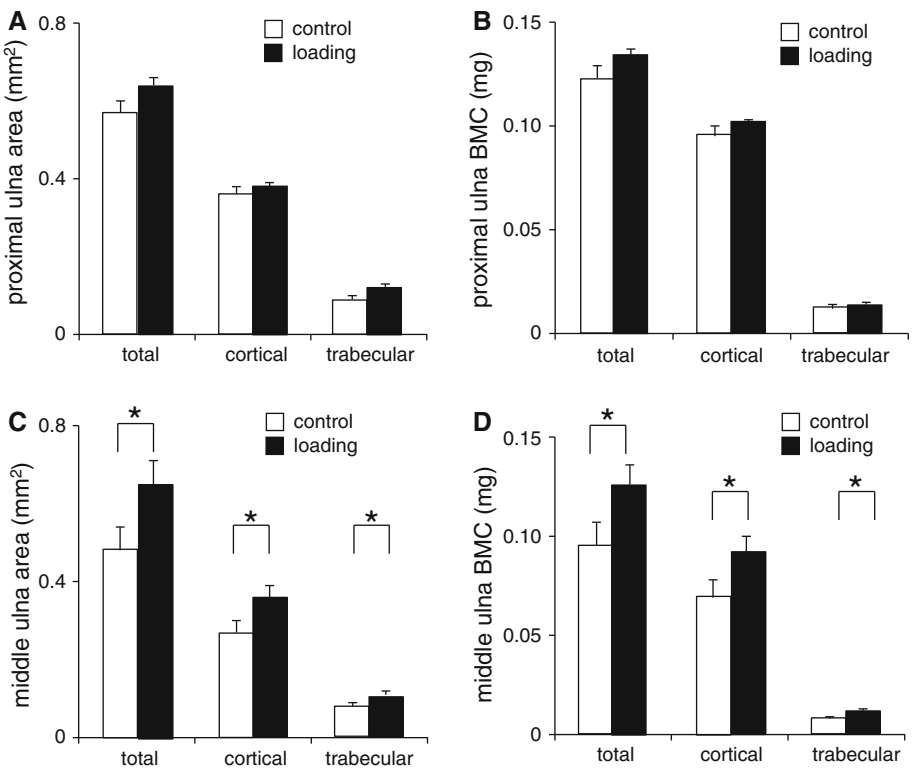

Fig. 7 Load-driven alterations of cortical bone and trabecular bone in the proximal and middle ulna. **a** Cross-sectional area in the proximal ulna. **b** BMC in the proximal ulna. **c** Cross-sectional area in the middle ulna. **d** BMC in the middle ulna

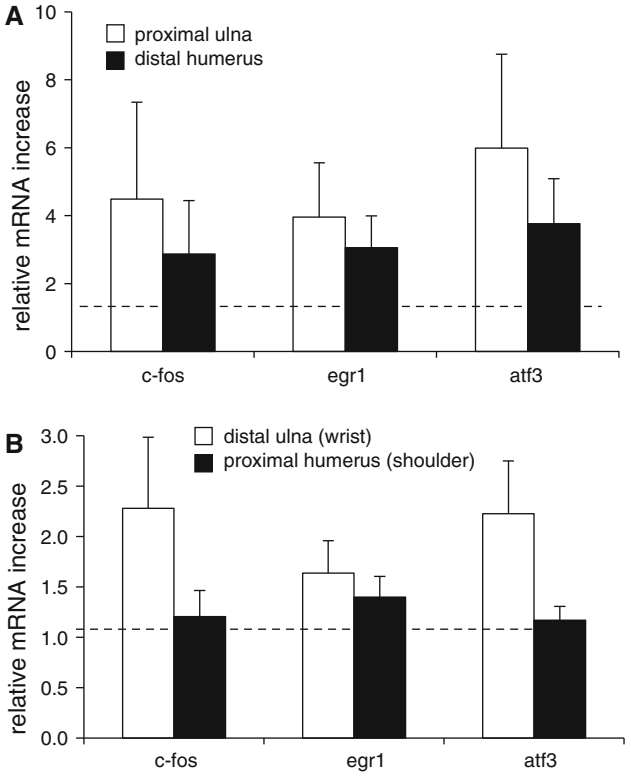

Fig. 8 Upregulation of the mRNA levels of stress-sensitive genes (c-fos, egr-1, and atf3) in the humerus and the ulna. **a** Messenger RNA expression levels at the loading site (proximal ulna and distal humerus). **b** Messenger RNA expression levels at the non-loading site (distal ulna—wrist, and proximal humerus—shoulder)

The results here are consistent with the proposed mechanism that dynamic tensile loads stimulate longitudinal bone formation of growing rodents, whereas compressive loads inhibit it. In our previous study, a three-dimensional strain distribution under static lateral loads was measured using electronic speckle-pattern interferometry [34]. In response to lateral loads applied to the knee ex vivo, the maximum strain at the loading site was in the order of a few millistrains and the strain at the midshaft cortical bone was in the order of 10 microstrains [23, 27]. The longitudinal strain along the bone length was positive, indicating that tensile force acts in the growth plate. As a biophysical mechanism for induction of bone formation with joint loading, it is proposed that alterations in intramedullary pressure are induced and interstitial molecular transport is activated by a dynamic pressure gradient [35–37]. To effectively lengthen long bones in the forelimb, further analysis is needed to examine the contribution of dynamic tensile stress along the length of the ulna and the humerus as well as alterations in intramedullary pressure. We observed differential sensitivity to elbow loading in the humerus and ulna. A potential factor for the observed difference may originate from anatomical dimensions and geometries, micrometric and nanometric structures in the lacunocanalicular network, and populations of osteocytes and osteoblasts. In the present study, the loading frequency is 5 Hz. Depending on loading frequencies, it might be possible that the humerus becomes more responsive to elbow loading that the ulna.

Molecular analysis showed that the selected early response genes (c-fos, egr1, and atf3) were upregulated in the loaded forelimb. It has been shown that these genes were upregulated at the loading sites with ankle loading and knee loading. Compared to the contralateral controls, the increases were 3–6 times in the proximal ulna and the distal humerus in which the loads were directly applied. Interestingly, the distal ulna (wrist) and the proximal humerus (shoulder), which did not receive direct loads, also presented increases in mRNA levels by 20–120%. These results are consistent with well-characterized remote influences of joint loading throughout the length of long bones, although the effects to the remote joints such as the wrist and shoulder are significantly smaller than those to the loaded elbow. Note that bone segments are a major contributor of mRNA expression, but the samples used in this study include articular cartilage and growth plates. Investigation of the effects of joint loading on gene expression in articular cartilage is an important subject to be conducted in future studies.

The understanding of the molecular mechanism for load-driven bone lengthening should facilitate development of a non-invasive loading strategy, which is free of pharmacological side-effects. Insulin-like growth factor 1 (IGF-1) is a key regulator in bone remodeling and repair [38–40], and its local administration is reported to lengthen rabbit tibiae [41]. Although approved and clinically applied, existing data for administration of human recombinant IGF-1 suggests occasional adverse effects including lymphoid hyperplasia, coarsening of the faces, and an increase in body fats as well as limitation of efficacy depending on individual patients [42–44]. Preliminary evaluation of gene expression with quantitative real-time PCR indicates that joint loading does not upregulate the mRNA level of IGF-1 in the loaded joint. Our previous study revealed that joint loading activated pathways involved in phosphoinositide 3-kinase, extracellular matrix-receptor interactions, transforming growth factor beta signaling, and Wnt signaling [26]. Further analyses are needed to determine the load-driven molecular pathway for longitudinal bone growth.

Load-induced longitudinal growth suppression has been reported to be proportional to load magnitude in the growing rat ulna [20, 21], but it is not known whether the change in growth rate is also proportional to the number of loading bouts per day or the number of loading days. It is conceivable that the rate of bone lengthening is dependent

on various loading conditions such as load magnitude, frequency in Hz, number of bouts per day, and loading duration in days as well as animal age. In summary, the current study demonstrates that elbow loading is an effective means to promote longitudinal bone growth in the mouse humerus and ulna. Joint loading may therefore be potentially useful for the development of load-driven therapies for limb length discrepancy and short stature.

Acknowledgments The authors thank G.M. Malacinski for critical reading of the manuscript. This study was supported by grants from the National Institute of Arthritis and Musculoskeletal and Skin Diseases Grant R03AR55322 (to P.Z.) and R01AR52144 (to H.Y.). The authors have no conflict of interest.

References

1. Vitale MA, Choe JC, Sesko AM, Hyman JE, Lee FY, Roye DP Jr, Vitale MG (2006) The effect of limb length discrepancy on health-related quality of life: is the '2 cm rule' appropriate? J Pediatr Orthop B 15:1–5
2. Bagatur AE, Doğan A, Zorer G (2002) Correction of deformities and length discrepancies of the forearm in children by distraction osteogenesis. Acta Orthop Traumatol Turc 36:111–116
3. White SC, Gilchrist LA, Wilk BE (2004) Asymmetric limb loading with true or simulated leg-length differences. Clin Orthop Relat Res 421:287–292
4. Rancont CM (2007) Chronic psoas syndrome caused by the inappropriate use of a heel lift. J Am Osteopath Assoc 107:415–418
5. Stanitski DF (1999) Limb-length inequality: assessment and treatment options. J Am Acad Orthop Surg 7:143–153
6. Friend L, Widmann RF (2008) Advances in management of limb length discrepancy and lower limb deformity. Curr Opin Pediatr 20:46–51
7. Birch JG, Samchukov ML (2004) Use of the Ilizarov method to correct lower limb deformities in children and adolescents. J Am Acad Orthop Surg 12:144–154
8. Fixsen JA (2003) Major lower limb congenital shortening: a mini review. J Pediatr Orthop B 12:1–12
9. Hantes ME, Malizos KN, Xenakis TA, Beris AE, Mavrodontidis AN, Soucacos PN (2001) Complications in limb-lengthening procedures: a review of 49 cases. Am J Orthop 30:479–483
10. Coppola C, Maffulli N (1999) Limb shortening for the management of leg length discrepancy. J R Coll Surg Edinb 44:46–54
11. Niedzielski K, Synder M, Borowski A (2002) Distraction epiphysiolysis in the treatment of uneven limb length. Ortop Traumatol Rehabil 30:459–463
12. Turner CH (2006) Bone strength: current concepts. Ann N Y Acad Sci 1068:429–446
13. Zuscik MJ, Hilton MJ, Zhang X, Chen D, O'Keefe RJ (2008) Regulation of chondrogenesis and chondrocyte differentiation by stress. J Chin Invest 118:429–438
14. Henderson ER, Feldman DS, Lusk C, van Bosse HJ, Sala D, Kummer FJ (2008) Conformational instability of the taylor spatial frame: a case report and biomechanical study. J Pediatr Orthop 28:471–477
15. Darling EM, Athanasiou KA (2003) Biomechanical strategies for articular cartilage regeneration. Ann Biomed Eng 31:1114–1124
16. Tanck E, Hannink G, Ruimerman R, Buma P, Burger EH, Huiskes R (2006) Cortical bone development under the growth plate is regulated by mechanical load transfer. J Anat 208:73–79
17. Stokes IA, Clark KC, Farnum CE, Aronsson DD (2007) Alterations in the growth plate associated with growth modulation by sustained compression or distraction. Bone 24:197–205
18. Stokes IA, Aronsson DD, Dimock AN, Cortright V, Beck S (2006) Endochondral growth in growth plates of three species at two anatomical locations modulated by mechanical compression and tension. J Orthop Res 24:1327–1334
19. Stokes IA, Gwadera J, Dimock A, Farnum CE, Aronsson DD (2005) Modulation of vertebral and tibial growth by compression loading: diurnal versus full-time loading. J Orthop Res 23:188–195
20. Ohashi N, Robling AG, Burr DB, Turner CH (2002) The effects of dynamic axial loading on the rat growth plate. J Bone Miner Res 17:284–292
21. Robling AG, Duijvelaar KM, Geevers JV, Ohashi N, Turner CH (2001) Modulation of appositional and longitudinal bone growth in the rat ulna by applied static and dynamic force. Bone 29:105–113
22. Yokota H, Tanaka SM (2005) Osteogenic potentials with joint-loading modality. J Bone Miner Metab 23:302–308
23. Zhang P, Tanaka SM, Jiang H, Su M, Yokota H (2006) Diaphyseal bone formation in murine tibiae in response to knee loading. J Appl Physiol 100:1452–1459
24. Zhang P, Sun Q, Turner CH, Yokota H (2007) Knee loading accelerates bone healing in mice. J Bone Miner Res 22:1979–1987
25. Zhang P, Yokota H (2007) Effects of surgical holes in mouse tibiae on bone formation induced by knee loading. Bone 40:1320–1328
26. Zhang P, Turner CH, Yokota H (2009) Joint loading-driven bone formation and signaling pathways predicted from genome-wide expression profiles. Bone 44:989–998
27. Zhang P, Tanaka S, Sun Q, Turner CH, Yokota H (2007) Frequency-dependent enhancement of bone formation in murine tibiae and femora with knee loading. J Bone Miner Metab 25:383–391
28. Zhang P, Su M, Tanaka S, Yokota H (2006) Knee loading causes diaphyseal cortical bone formation in murine femurs. BMC Musculoskelet Dis 73:1–12
29. Zhang P, Hamamura K, Turner CH, Yokota H (2010) Lengthening of mouse hindlimbs with joint loading. J Bone Miner Metab 28:268–275
30. Evans KD, Lau ST, Oberbauer AM, Martin RB (2003) Alendronate affects long bone length and growth plate morphology in the oim mouse model for Osteogenesis Imperfecta. Bone 32:268–274
31. Shin HD, Yang KJ, Park BR, Son CW, Jang HJ, Ku SK (2007) Antiosteoporotic effect of Polycan, beta-glucan from Aureobasidium, in ovariectomized osteoporotic mice. Nutrition 23:853–860
32. Govoni KE, Wergedal JE, Chadwick RB, Srivastava AK, Mohan S (2008) Prepubertal OVX increases IGF-I expression and bone accretion in C57BL/6J mice. Am J Physiol Endocrinol Metab 295:E1172–E7780
33. Soon G, Quintin A, Scalfo F, Antille N, Williamson G, Offord E, Ginty F (2006) PIXImus bone densitometer and associated technical measurement issues of skeletal growth in the young rat. Calcif Tissue Int 78:186–192
34. Yang L, Zhang P, Liu S, Samala P, Yokota H (2007) Measurement of strain distributions in mouse femora with 3D-digital speckle pattern interferometry. Opt Laser Eng 45:843–851
35. Zhang P, Su M, Liu Y, Hus A, Yokota H (2007) Knee loading dynamically alters intramedullary pressure in mouse femora. Bone 40:538–543
36. Su M, Jiang H, Zhang P, Liu Y, Wang E, Hsu A, Yokota H (2006) Load-driven molecular transport in mouse femur with knee-loading modality. Ann Biomed Eng 34:1600–1606

37. Zhang P, Malacinski GM, Yokota H (2008) Joint loading modality: its application to bone formation and fracture healing. Br J Sport Med 42:556–560
38. Fowlkes JL, Thraikill KM, Liu L, Wahl EC, Bunn RC, Cockrell GE, Perrien DS, Aronson J, Lumpkin CK Jr (2006) Effects of systemic and local administration of recombinant human IGF-I (rhIGF-I) on de novo bone formation in an aged mouse model. J Bone Miner Res 21:1359–1366
39. Suzuki S, Itoh K, Ohyama K (2004) Local administration of IGF-I stimulates the growth of mandibular condyle in mature rats. J Orthod 31:138–143
40. Reijinders CM, Bravenboer N, Tromp AM, Blankenstein MA, Lips P (2007) Effect of mechanical loading on insulin-like growth factor-I gene expression in rat tibia. J Endocrinol 192:131–140
41. Abbaspour A, Takata S, Matsui Y, Katoh S, Takahashi M, Yasui N (2008) Continuous infusion of insulin-like growth factor-I into the epiphysis of the tibia. Int Orthop 32:395–402
42. Rosenbloom AL (2007) The role of recombinant insulin-like growth factor I in the treatment of the short child. Curr Opin Pediatr 19:458–464
43. Rosenbloom AL (2006) Is there a role for recombinant insulin-like growth factor-I in the treatment of idiopathic short stature? Lancet 368:612–616
44. Rosenbloom AL, Guevara-Aguirre J (2006) Controversy in clinical endocrinology: reclassification of insulin-like growth factor I production and action disorders. J Clin Endocrinol Metab 91:4232–4234